Zeitschrift: IABSE publications = Mémoires AIPC = IVBH Abhandlungen
Band: 31 (1971)

Artikel: Stiffened plates in unaxial compression
Autor: Sherbourne, A.N. / Liaw, C.Y. / Marsh, C.
DOI: https://doi.org/10.5169/seals-24213

Stiffened Plates in Uniaxial Compression

Plaques renforcées lors de compression mono-axiale

Versteifte Platten bei einachsigem Zusammendrücken

A. N. SHERBOURNE
Professor of Civil Engr. and Dean, Faculty of Engr., Univ. of Waterloo; currently Visiting Prof., LNEC, Lisbon, Portugal

C. Y. LIAW
Formerly Graduate Student, Dept. of Civil Engr., Univ. of Waterloo, Ontario, Canada

C. MARSH
Associate Professor of Civil Engr., Sir George Williams Univ., Montreal, Quebec, Canada

Introduction

Previous papers [1, 2] dealt with the ultimate strength of the plane, rectangular plate loaded in uniaxial compression. A critical review of the literature was presented along with a possible physical explanation of the build-up of stresses in the plate in the region of transition from elastic loading, associated with post-buckling stability, to plastic unloading associated with geometry change accompanying a kinematic mechanism.

The stiffened plate, whose ultimate strength is to be determined as part of this investigation, possesses different rigidities in two orthogonal directions; the load is applied in the stronger direction. Typical examples of this property are to be found in the longitudinally stiffened or corrugated plate. The physical behaviour of this element is similar to that of the plane plate described previously, except for the relative importance of the various stress components generated. After initial buckling, the transverse membrane stresses are small in a corrugated plate yet are significant in a stiffened panel. A second point of difference between the stiffened and unstiffened elements is the nature of the plastic mechanism which emerges in the former. For a longitudinally stiffened plate the pattern of plastic buckling will approach a series of simple columns restrained by transverse membrane action but not by transverse bending which, in all cases, is small.

Elastic Loading

1. Assumptions

The investigation involves the elastic behaviour of a stiffened plate, simply supported along four sides, which is compressed in the stronger direction, i.e., the direction of greater rigidity. In considering this problem, the following assumptions are made:

1. The plate possesses infinite elasticity, in terms of its stress-strain relationship, for the calculation of the loading line and perfect plasticity for purposes of the mechanism.
2. Initial imperfections are neglected.
3. The load is applied uniformly and normal to the top and bottom edges of the plate.
4. For the buckled plate, each half-wave can be considered as simply supported.
5. The edges are assumed to remain straight.
6. The strains in post-buckling are accurately prescribed by first and second order terms in the displacements.

2. Buckling Stress

The plate has coordinates as shown in Fig. 1. To establish the buckling stress, the deflection is assumed to be infinitesimal so that the loads per unit width, N_x, N_y, N_{xy} are constant and uniform within the plate.

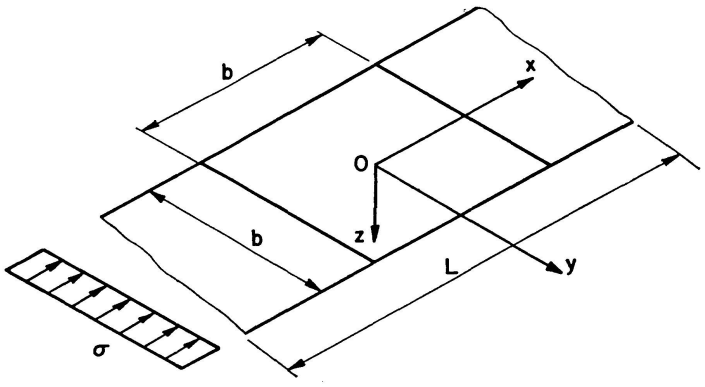

Fig. 1. Coordinate System.

The bending strains at distance z from the neutral axis are

$$\epsilon_x = \frac{z}{\rho_x}, \qquad \epsilon_y = \frac{z}{\rho_y},$$

where $1/\rho_x$, $1/\rho_y$ denote the curvatures of this neutral surface in the xz and yz planes, respectively. From Hooke's law

$$\epsilon_x = \frac{\sigma_x}{E_x} - \mu_y \frac{\sigma_y}{E_y}, \qquad \epsilon_y = \frac{\sigma_y}{E_y} - \mu_x \frac{\sigma_x}{E_x}, \qquad \tau_{xy} = G_{xy}\gamma_{xy},$$

where μ_x and μ_y are directional values of Poisson's ratio and E_x, E_y and G_{xy} represent elastic and shear moduli respectively associated with x and y. It follows that

$$\frac{z}{\rho_x} = \frac{\sigma_x}{E_x} - \mu_y \frac{\sigma_y}{E_y}, \qquad \frac{z}{\rho_y} = \frac{\sigma_y}{E_y} - \mu_x \frac{\sigma_x}{E_x}. \tag{1}$$

The stresses, moments and curvatures are coupled thus:

$$\begin{aligned} \sigma_x &= \frac{M_x z}{I_x}, & \sigma_y &= \frac{M_y z}{I_y}, \\ \frac{1}{\rho_x} &= -\frac{\partial^2 \omega}{\partial x^2}, & \frac{1}{\rho_y} &= -\frac{\partial^2 \omega}{\partial y^2}, \\ \gamma_{xy} &= -2 G_{xy} z \frac{\partial^2 \omega}{\partial x \, \partial y}, \\ M_{xy} &= -\int_A \gamma_{xy} z \, dA = 2 G_{xy} I_{xy} \frac{\partial^2 \omega}{\partial x \, \partial y}, \end{aligned} \tag{2}$$

where ω is the deflection of the plate. The moment-curvature relationships become

$$\begin{aligned} \frac{\partial^2 \omega}{\partial x^2} &= -\frac{M_x}{E_x I_x} + \mu_y \frac{M_y}{E_y I_y}, \\ \frac{\partial^2 \omega}{\partial y^2} &= -\frac{M_y}{E_y I_y} + \mu_x \frac{M_x}{E_x I_x}, \\ \frac{\partial^2 \omega}{\partial x \, \partial y} &= \frac{1}{2 G_{xy} I_{xy}} M_{xy}. \end{aligned} \tag{3}$$

Solving Eq. (3) leads to

$$\begin{aligned} M_x &= -\frac{E_x I_x}{1 - \mu_x \mu_y} \left(\frac{\partial^2 \omega}{\partial x^2} + \mu_x \frac{\partial^2 \omega}{\partial y^2} \right), \\ M_y &= -\frac{E_y I_y}{1 - \mu_x \mu_y} \left(\frac{\partial^2 \omega}{\partial y^2} + \mu_y \frac{\partial^2 \omega}{\partial x^2} \right), \\ M_{xy} &= 2 G_{xy} I_{xy} \frac{\partial^2 \omega}{\partial x \, \partial y}. \end{aligned} \tag{4}$$

Writing

$$\begin{aligned} D_1 &= \frac{E_x I_x}{1 - \mu_x \mu_y}, & D_2 &= \frac{E_y I_y}{1 - \mu_x \mu_y}, \\ D_3 &= \frac{1}{2}(\mu_x D_2 + \mu_y D_1) + 2 G_{xy} I_{xy} \end{aligned} \tag{5}$$

and substituting into (4) and differentiating, obtain

$$\begin{aligned} \frac{\partial^2 M_x}{\partial x^2} &= -D_1 \left(\frac{\partial^4 \omega}{\partial x^4} + \mu_y \frac{\partial^4 \omega}{\partial x^2 \, \partial y^2} \right), \\ \frac{\partial^2 M_y}{\partial y^2} &= -D_2 \left(\frac{\partial^4 \omega}{\partial y^4} + \mu_x \frac{\partial^4 \omega}{\partial x^2 \, \partial y^2} \right), \\ \frac{\partial^2 M_{xy}}{\partial x \, \partial y} &= \left[D_3 - \frac{1}{2}(\mu_x D_2 + \mu_y D_1) \right] \frac{\partial^4 \omega}{\partial x^2 \, \partial y^2}. \end{aligned}$$

For a stiffened or corrugated plate one can assume μ_x, μ_y equal to zero [2] leading to

$$\frac{\partial^2 M_x}{\partial x^2} - 2\frac{\partial^2 M_{xy}}{\partial x \partial y} + \frac{\partial^2 M_y}{\partial y^2} = -D_1\frac{\partial^4 \omega}{\partial x^4} - D_2\frac{\partial^4 \omega}{\partial y^4} - 2D_3\frac{\partial^4 \omega}{\partial x^2 \partial y^2}. \tag{6}$$

The equation of equilibrium for plates is given as [2]

$$\frac{\partial^2 M_x}{\partial x^2} - 2\frac{\partial^2 M_{xy}}{\partial x \partial y} + \frac{\partial^2 M_y}{\partial y^2} = -\left(q + N_x\frac{\partial^2 \omega}{\partial x^2} + N_y\frac{\partial^2 \omega}{\partial y^2} + 2N_{xy}\frac{\partial^2 \omega}{\partial x \partial y}\right). \tag{7}$$

Since the plate under consideration suffers pure compression in the direction x, $q = N_y = N_{xy} = 0$, from which

$$D_1\frac{\partial^4 \omega}{\partial x^4} + 2D_3\frac{\partial^4 \omega}{\partial x^2 \partial y^2} + D_2\frac{\partial^4 \omega}{\partial y^4} = -N_x\frac{\partial^2 \omega}{\partial x^2}. \tag{8}$$

Assuming the plate buckles into m half-waves in the x direction and only one half-wave in y, then transverse deflection can be represented by

$$w = \delta \cos\frac{m\pi x}{a}\cos\frac{\pi y}{b}, \tag{9}$$

where a is the half wavelength in the x-direction. Substituting into (8) leads to

$$N_x = \frac{\pi^2}{b}\left[D_1\left(\frac{m b}{a}\right)^2 + 2D_3 + D_2\left(\frac{a}{m b}\right)^2\right]$$

or

$$(\sigma_x)_{cr} = \frac{\pi^2}{b^2 t'}\left[D_1\left(\frac{m b}{a}\right)^2 + 2D_3 + D_2\left(\frac{a}{m b}\right)^2\right], \tag{10}$$

where $t' = A/b$, A is the cross-sectional area of the plate and b is the width. This equation can be written in the form

$$\sigma_{cr} = K\frac{\pi^2 D_1}{b^2 t'},$$

where

$$K = \left(\frac{m b}{a}\right)^2 + 2\frac{D_3}{D_1} + \frac{D_2}{D_1}\left(\frac{a}{m b}\right)^2. \tag{11}$$

Values of K are plotted in Fig. 2 against aspect ratio a/b. The intersection of m and $(m+1)$ half waves is at

$$\frac{a}{b} = \beta\sqrt{m(m+1)},$$

where

$$\beta = \left(\frac{D_1}{D_2}\right)^{1/4}.$$

Assuming $m = 1$, the smallest value of critical stress is obtained when

$$\frac{\partial \sigma_{cr}}{\partial\left(\frac{b}{a}\right)} = 0 \quad \text{or} \quad \frac{a}{b} = \sqrt[4]{\frac{D_1}{D_2}} = \beta.$$

βb is thus the length of one half wave and the critical stress becomes

$$\sigma_{cr} = \frac{2\pi^2}{b^2 t'}[(D_1 D_2)^{1/2} + D_3]. \tag{12}$$

This case is represented by point A in Fig. 2.

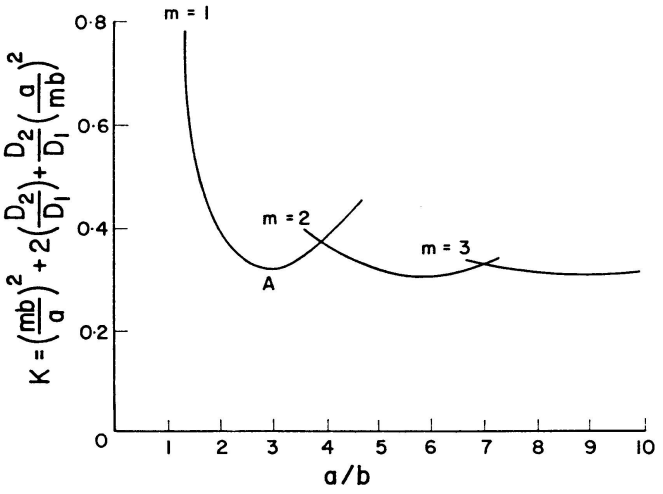

Fig. 2. Buckling Coefficients for Simply Supported Stiffened Plate.

In the case of a stiffened flat plate one may assume $I_y = \frac{t^3}{12(1-\mu^2)}$, where t is the thickness of plate and μ is Poisson's ratio for the material assumed independent of direction and having a value of approximately 0.3. Thus

$$\beta = 1.8\left(\frac{I_x}{t^3}\right)^{1/4}.$$

In the case of a corrugated plate

$$I_x = \frac{A}{b} r_x^2 = \eta t r_x^2,$$

where $$\eta = \frac{A}{bt} = \frac{t'}{t}$$

and $$I_y = \frac{t^3}{12(1-\mu^2)\eta},$$

leading to $$\beta = 1.8\left(\eta \frac{r_x}{t}\right)^{1/2},$$

where r_x is a radius of gyration of the section.

If torsional effects are neglected and $\mu_x = \mu_y = 0$, then, for a long plate, i. e., $a > \beta b$, from (10)

$$\sigma_{cr} = \frac{2\pi^2}{b^2 t'} \frac{E I_x}{\beta^2 (1 - \mu_x \mu_y)} = \frac{2\pi^2 E I_x}{b^2 t' \beta^2}$$

or $$\sigma_{cr} = \frac{\pi^2 E}{\lambda^2}, \tag{13a}$$

where $$\lambda = \left(\frac{b^2\beta^2}{2r_x^2}\right)^{1/2} = 0.7\frac{b\beta}{r_x}.$$

For a short plate i.e., $a < \beta b$

$$\sigma_{cr} = \frac{\pi^2 E}{\lambda^2} = \frac{\pi^2}{b^2 t'}\left[D_1\left(\frac{b}{a}\right)^2 + \frac{D_1}{\beta^4}\left(\frac{a}{b}\right)^2\right] = \frac{\pi^2 E I_x}{a^2 t'}\left(1 + \frac{a^4}{\beta^4 b^4}\right), \tag{13b}$$

where $$\lambda = \frac{1}{\left[1 + \left(\frac{a}{\beta b}\right)^4\right]^{1/2}}\frac{a}{r_x}.$$

One may conclude that the value of the critical stress for a corrugated or stiffened flat plate, compressed longitudinally, is given by the following equations:

$$\sigma_{cr} = \frac{\pi^2 E}{\lambda^2},$$

where $$\lambda = 0.7\frac{b\beta}{r_x} \quad \text{for } a > \beta b$$

and $$\lambda = \frac{1}{\left[1 + \left(\frac{a}{\beta b}\right)^4\right]^{1/2}}\frac{a}{r_x} \quad \text{for } a < \beta b.$$

The aspect ratio is

$\beta = 1.8\left(\eta\frac{r_x}{t}\right)^{1/2}$ for the corrugated plate,

$\beta = 1.8\left(\frac{I_x}{t^3}\right)^{1/4}$ for the longitudinally stiffened plate.

3. Post-buckling Behaviour

The energy method is used to derive the relationship between load and central deflection of the plate assumed to buckle in one half wave only. The deflected shape of the plate is given by the following

$$\omega = \delta \cos\frac{\pi x}{a}\cos\frac{\pi y}{b},$$

which satisfies the boundary conditions of a simply supported plate, i.e.,

at $x = 0, \quad y = 0, \qquad \omega = \delta, \qquad \frac{\partial\omega}{\partial x} = \frac{\partial\omega}{\partial y} = 0,$

at $x = \pm\frac{a}{2}, \qquad \omega = \frac{\partial^2\omega}{\partial x^2} = 0,$

$y = \pm\frac{b}{2}, \qquad \omega = \frac{\partial^2\omega}{\partial y^2} = 0.$

Since the edges are assumed to be straight, the displacement components u and v in the middle plane of the plate, corresponding to x and y directions, can be chosen as

$$\begin{aligned} u &= B \sin\frac{2\pi x}{a}\cos\frac{\pi y}{b} + i\,x, \\ v &= C \sin\frac{2\pi y}{b}\cos\frac{\pi x}{a} + j\,y, \end{aligned} \tag{14}$$

where B, C, i, j are coordinate functions. The second part of the expressions correspond to uniform movement of the boundaries.

The components of strain at the median surface of the plate are

$$\begin{aligned} \epsilon_x &= \frac{\partial u}{\partial x} + \frac{1}{2}\left(\frac{\partial \omega}{\partial x}\right)^2, \\ \epsilon_y &= \frac{\partial v}{\partial y} + \frac{1}{2}\left(\frac{\partial \omega}{\partial y}\right)^2, \\ \gamma_{xy} &= \frac{\partial v}{\partial x} + \frac{\partial u}{\partial y} + \frac{\partial \omega}{\partial x}\frac{\partial \omega}{\partial y}. \end{aligned} \tag{15}$$

The corresponding membrane strain energy is

$$V_M = \frac{t}{2}\int_{-b/2}^{b/2}\int_{-a/2}^{a/2}(\eta\,\sigma_x\epsilon_x + \sigma_y\epsilon_y + \tau_{xy}\gamma_{xy})\,dx\,dy.$$

For a corrugated or stiffened plate $\mu_x = \mu_y = 0$, as before, such that

$$\sigma_x = E_x\epsilon_x, \qquad \sigma_y = E_y\epsilon_y \quad \text{and} \quad \tau_{xy} = G_{xy}\gamma_{xy}$$

and

$$V_M = \frac{t}{2}\int_{-b/2}^{b/2}\int_{-a/2}^{a/2}(\eta\,E_x\epsilon_x^2 + E_y\epsilon_y^2 + G_{xy}\gamma_{xy}^2)\,dx\,dy. \tag{16}$$

The strain energy of bending is

$$V_B = -\frac{1}{2}\int_{b/2}^{b/2}\int_{a/2}^{a/2}\left(M_x\frac{\partial^2\omega}{\partial x^2} + M_y\frac{\partial^2\omega}{\partial y^2} + 2\,M_{xy}\frac{\partial^2\omega}{\partial x\,\partial y}\right)dx\,dy$$

and substituting from (4), (5) into the above, leads to

$$V_B = \frac{1}{2}\int_{-b/2}^{b/2}\int_{-a/2}^{a/2}\left[D_1\left(\frac{\partial^2\omega}{\partial x^2}\right)^2 + D_2\left(\frac{\partial^2\omega}{\partial y^2}\right)^2 + 4\,G_{xy}\,I_{xy}\left(\frac{\partial^2\omega}{\partial x\,\partial y}\right)^2\right]dx\,dy. \tag{17}$$

The final forms of membrane and bending energy are obtained by substituting equations (9), (14) and (15) into (16) and (17), separately to yield

$$V_M = \frac{t}{2}\Big\{\eta E_x\left[\frac{\pi^2 b}{a}\left(B^2+\frac{i}{4}\delta^2-\frac{2}{3}B\frac{\delta^2}{a}\right)+ab\left(i+\frac{9\pi^4}{256a^4}\delta^4\right)\right]$$
$$+E_y\left[\frac{\pi^2 a}{b}\left(C^2+\frac{j}{4}\delta^2-\frac{2}{3}C\frac{\delta^2}{b}\right)+ab\left(j+\frac{9\pi^4}{256b^4}\delta^4\right)\right] \tag{18}$$
$$+G_{xy}\left[\frac{\pi^2}{4}\left(\frac{a}{b}\right)B^2+\frac{\pi^2}{4}\left(\frac{b}{a}\right)C^2+\frac{\pi^4\delta^4}{64ab}+\frac{32}{9}BC-\pi^2\frac{aB+bC}{3ab}\delta^2\right]\Big\},$$

$$V_B = \frac{\pi^4}{4}ab\delta^2\left[\frac{D_1}{2a^4}+\frac{D_2}{2b^4}+\frac{2D_3-2G_{xy}I_{xy}}{a^2b^2}\right]. \tag{19}$$

The work done by the external load is given by

$$V_E = -2\int_{-b/2}^{b/2} p\,u|_{x=a/2}\,dy = -P\,i\,a, \tag{20}$$

where p is the applied load per unit width, while P is the total load. The total energy of the plate may be written as the summation of V_E, V_B and V_M.

$$V = V_E + V_B + V_M.$$

In accordance with the theory of Minimum Potential Energy, post-buckling equilibrium is governed by

$$\frac{\partial V}{\partial B} = \frac{\partial V}{\partial C} = \frac{\partial V}{\partial \delta} = 0. \tag{21}$$

Furthermore, for a virtual displacement, the internal and external works are identical, i.e., $p\,\delta u = \delta(V_B + V_M)$. Differentiating with respect to i, leads to

$$\frac{\partial}{\partial i}(V_B + V_M - pu) = 0 \quad \text{or} \quad \frac{\partial V}{\partial i} = 0. \tag{22}$$

From Eqs. (21) and (22), the following four equations are obtained

$$\frac{\partial V}{\partial B} = 0 = \frac{t}{2}\Big\{\eta E_x\left[\frac{\pi^2 b}{a}\left(2B-\frac{2\delta^2}{3a}\right)\right]-G_{xy}\left[\frac{\pi^2}{2}\frac{a}{b}B+\frac{32}{9}C-\frac{\pi^2}{3}\frac{\delta^2}{b}\right]\Big\}, \tag{a}$$

$$\frac{\partial V}{\partial C} = 0 = \frac{t}{2}\Big\{E_y\left[\frac{\pi^2 a}{b}\left(2C-\frac{2\delta^2}{3b}\right)\right]+G_{xy}\left[\frac{\pi^2}{2}\frac{b}{a}C+\frac{32}{9}B-\frac{\pi^2\delta^2}{3a}\right]\Big\}, \tag{b}$$

$$\frac{\partial V}{\partial \delta} = 0 = \frac{t}{2}\Big\{\eta E_x\left[\frac{\pi^2 b}{a}\left(\frac{i}{2}\delta-\frac{4}{3}\frac{\delta}{a}B\right)+\frac{9\pi^4 b}{64}\left(\frac{\delta}{a}\right)^3\right]$$
$$+E_y\left[\frac{\pi^2 a}{b}\left(\frac{j}{2}\delta-\frac{4}{3}\frac{\delta}{a}C\right)+\frac{9\pi^4 a}{64}\left(\frac{\delta}{b}\right)^3\right] \tag{c}$$
$$+G_{xy}\left[\frac{\pi^4}{16ab}\delta^3-\frac{2}{3}\pi^2\frac{aB+bC}{ab}\delta\right]+\frac{\pi^4}{4}\frac{D_1}{ab}\delta K\Big\}$$

$$\frac{\partial V}{\partial i} = 0 = E_x\eta tb\left[\frac{\pi^2}{8}\frac{\delta^2}{a}+ai\right]-Pa. \tag{d}$$

The value of j is derived from the condition that the applied force at two boundaries is zero, i.e.,

$$P_y = 0 = \int_{-a/2}^{a/2} \sigma_y|_{b/2}\, t\, dx = t\, E_y \int_{-a/2}^{a/2} \epsilon_y\, dx = t\, E_y \left[j\, a + \frac{4\, a\, C}{b} \cos \frac{2\pi y}{b} + \frac{\pi^2}{4} \frac{a}{b^2} \delta^2 \sin^2 \frac{\pi y}{b} \right],$$

such that

$$j = \frac{4\, C}{b} - \frac{\pi^2 \delta^2}{4\, b^2}. \tag{e}$$

From (a) and (b)

$$C = \frac{0.46\, G_{xy}^2 + 1.33\, \eta\, E_x E_y + \left[4.21 \left(\frac{b}{a}\right)^2 \eta\, E_x + 3.29 \left(\frac{a}{b}\right)^2 E_x \right] G_{xy}}{1.20\, G_{xy}^2 + 39.4\, \eta\, E_x E_y + \left[9.85 \left(\frac{b}{a}\right)^2 \eta\, E_x + 9.85 \left(\frac{a}{b}\right)^2 E_y \right] G_{xy}} \frac{\delta^2}{b},$$

$$B = \frac{0.46\, G_{xy}^2 + 1.33\, \eta\, E_x E_y + \left[3.29 \left(\frac{b}{a}\right)^2 \eta\, E_x + 4.21 \left(\frac{a}{b}\right)^2 E_y \right] G_{xy}}{1.20\, G_{xy}^2 + 39.4\, \eta\, E_x E_y + \left[9.85 \left(\frac{b}{a}\right)^2 \eta\, E_x + 9.85 \left(\frac{a}{b}\right)^2 E_y \right] G_{xy}} \frac{\delta^2}{a},$$

while from (c)

$$i = \frac{8\, B}{a} - \frac{\pi^2 D_1 K}{b^2 t\, \eta\, E_x} - \frac{4\, C}{3\, b} \left(\frac{a}{b}\right)^2 \frac{E_y}{\eta\, E_x} - \frac{9}{32} \frac{\pi^2}{a^2} \delta^2 - \frac{\pi^2}{32} \frac{a^2}{b^4} \delta^2 \frac{E_y}{\eta\, E_x} - \frac{\pi^2}{8\, b^2} \delta^2 \frac{G_{xy}}{\eta\, E_x} + \frac{4}{3} \frac{a\, B + b\, C}{b^2} \frac{G_{xy}}{\eta\, E_x}.$$

Substituting C and B into the expression for i leads to

$$\begin{aligned} i = -\frac{\pi^2 D_1 K}{b^2 t\, \eta\, E_x} - \frac{\delta^2}{b^2} & \frac{1}{1.20\, G_{xy}^2 + 39.4\, \eta\, E_x E_y + 9.85 \left[\left(\frac{b}{a}\right)^2 \eta\, E_x + \left(\frac{a}{b}\right)^2 E_y \right] G_{xy}} \\ & \cdot \left\{ \left[4.29 \left(\frac{b}{a}\right)^2 + 3.184 \left(\frac{a}{b}\right)^2 \frac{E_y}{\eta\, E_x} + 0.255 \frac{G_{xy}}{\eta\, E_x} \right] G_{xy}^2 \right. \\ & + \left[105.5 \left(\frac{b}{a}\right)^2 + 13.98 \left(\frac{a}{b}\right)^2 \frac{E_y}{\eta\, E_x} + 69.85 \frac{G_{xy}}{\eta\, E_x} \right] \eta\, E_x E_y \\ & \left. + \left[18.62 \left(\frac{b}{a}\right)^2 + 7.43 \left(\frac{a}{b}\right)^2 \left(\frac{E_y}{\eta\, E_x}\right)^2 \right] \eta\, E_x G_{xy} \right\}. \end{aligned}$$

Substituting the expression for i into Eq. (d) yields a load-deflexion relationship,

$$\begin{aligned} P = -\frac{\pi^2 D_1 K}{b} - \frac{\delta^2}{b^2} & E_x \eta\, t\, b \frac{1}{1.20\, G_{xy}^2 + 39.4\, \eta\, E_x E_y + 9.85 \left[\left(\frac{b}{a}\right)^2 \eta\, E_x + \left(\frac{a}{b}\right)^2 E_y \right] G_{xy}} \\ & \cdot \left\{ \left[2.81 \left(\frac{b}{a}\right)^2 + 3.184 \left(\frac{a}{b}\right)^2 \frac{E_y}{\eta\, E_x} + 0.255 \frac{G_{xy}}{\eta\, E_x} \right] G_{xy}^2 \right. \\ & + \left[57.0 \left(\frac{b}{a}\right)^2 + 13.98 \left(\frac{a}{b}\right)^2 \frac{E_y}{\eta\, E_x} + 57.75 \frac{G_{xy}}{\eta\, E_x} \right] \eta\, E_x E_y \\ & \left. + \left[6.47 \left(\frac{b}{a}\right)^4 + 7.43 \left(\frac{a}{b}\right)^4 \left(\frac{E_y}{\eta\, E_x}\right)^2 \right] \eta\, E_x G_{xy} \right\}. \end{aligned} \tag{23}$$

4. *Analytical Results*

a) Zero Transverse Plate Stiffness (Corrugated Plate). If it is assumed that the elastic modulus in the transverse direction of a corrugated plate is very small, i.e., $E_y = 0$, Eq. (23) reduces to

$$P = -\frac{\pi^2 D_1 K}{b} - \frac{E_x \eta t}{b} \frac{2.81\left(\frac{b}{a}\right)^2 G_{xy} + 0.255 \frac{G_{xy}^2}{\eta E_x} + 6.47\left(\frac{b}{a}\right)^2 \eta E_x}{1.20\, G_{xy} + 9.85\, \eta \left(\frac{b}{a}\right)^2 E_x} \delta^2.$$

Taking $E_x = E$, $G_{xy} = \dfrac{E}{2(1+\mu)}$ and $\mu = 0.3$.

$$P = -\frac{\pi^2 D_1 K}{b} - E \eta t b \frac{6.47\, \eta \left(\frac{b}{a}\right)^2 + \frac{0.036}{\eta}\left(\frac{a}{b}\right)^2 + 1.06}{0.451\left(\frac{a}{b}\right)^2 + 9.87\, \eta} \left(\frac{\delta}{b}\right)^2. \tag{23a}$$

b) Finite Transverse Plate Stiffness (Corrugated Plate). If the transverse membrane stress is not negligible, the value of E_y should be determined. It is assumed that the fold angle for the corrugation, θ, does not change under load. Then, to find the effective modulus, the problem can be treated as involving a linearly loaded folded plate (Fig. 3).

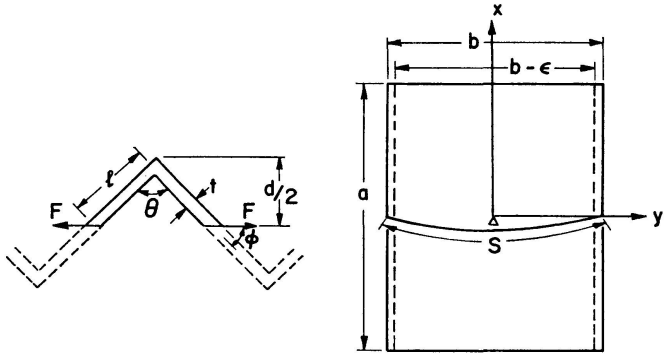

Fig. 3. Corrugated Plate.

The deformation in the direction of F (the membrane force per unit width) is

$$\delta = \frac{F l}{E t} \cos^2 \phi + \frac{F l^3}{3 E I} \sin^2 \phi.$$

The strain in the direction of F thus becomes

$$\epsilon = \frac{F}{E t} \cos \phi + \frac{4 F l^2}{E t^3} \frac{\sin^2 \phi}{\cos \phi} = \frac{F \cos \phi}{E t} \left[1 + 4\left(\frac{l}{t}\right)^2 \tan^2 \phi\right],$$

such that

$$E_y = \frac{E}{\cos^2 \phi \left[1 + 4\left(\frac{l}{t}\right)^2 \tan^2 \phi\right]},$$

but $$\eta = \frac{t'}{t} = \frac{1}{\cos\phi} \quad \text{and} \quad l\sin\phi = \frac{d}{2},$$

hence $$E_y = \frac{E\eta^2}{1+\eta^2\left(\frac{d}{t}\right)^2},$$

where E is the elastic modulus of the material and η is the ratio of developed to net width. With the value of E_y and Eq. (23), it is possible to obtain the load-deflection equation for the case of small transverse membrane stress for which the assumption that θ = constant is valid.

c) Zero Edge Transverse Stress (Corrugated Plate). Eq. (23) is derived under the assumption that the supported edges remain straight and there is a transverse membrane stress distributed along the supported edges. In most test specimens, however, such as the tube tests, the supported edges are free of stress if the shear stress is neglected. A modification of Eq. (23) can be made by assuming the transverse membrane stress obeys the function

$$\sigma_y = \sigma_y^0 \cos\frac{2\pi x}{a}\cos\frac{\pi y}{b}.$$

The coefficient σ_y^0, which is the transverse membrane stress at the center of the plate, can be found from the assumption that the supported edges remain straight. Therefore, the transverse shortening due to the pure compression at $x=a/2$ i. e., the loaded edge, is equal to the transverse shortening at $x=0$ (Fig. 3b), i. e., the section of maximum lateral deflection. At $x=a/2$, the total transverse shortening is

$$\epsilon = \int_{-b/2}^{b/2} \epsilon_y = \frac{1}{E_y}\int_{-b/2}^{b/2} \sigma_y^0 \cos\frac{\pi y}{b}\,dy = \frac{2b}{\pi}\frac{\sigma_y^0}{E_y}.$$

At $x=0$, the transverse mid-plane length becomes

$$S = b + \int_{-b/2}^{b/2} \epsilon_y|_{x=0}\,dy = b + \frac{1}{E_y}\int_{-b/2}^{b/2} \sigma_y^0 \cos\frac{\pi y}{b}\,dy = b + \frac{2b}{\pi}\frac{\sigma_y^0}{E_y}.$$

Now $$S-(b-\epsilon) = \frac{1}{2}\int_{-b/2}^{b/2}\left(\frac{d\omega}{dy}\right)_{x=0} dy = \left(\frac{\pi}{b}\right)^2\frac{\delta^2 b}{4}.$$

Substituting the expressions for ϵ and S into the above equation gives

$$\sigma_y^0 = \frac{\pi^3}{16}E_y\left(\frac{\delta}{b}\right)^2.$$

The membrane strain due to the transverse membrane stress in Eq. (18), i. e., the term with the coefficient E_y, should be replaced by the following expression

$$\frac{t}{2E_y}\int_{-b/2}^{b/2}\int_{-a/2}^{a/2}\sigma_y^2\,dx\,dy=\frac{t(\sigma_y^0)^2}{2E_y}\int_{-b/2}^{b/2}\int_{-a/2}^{a/2}\left(\cos\frac{2\pi x}{a}\cos\frac{\pi y}{b}\right)^2 dx\,dy=\frac{\pi^6 E_y t}{2048}ab\left(\frac{\delta}{b}\right)^4.$$

After replacing this term in Eq. (18), we may obtain B, C, and i from a similar procedure as used previously. The final results are

$$B=\frac{\pi^2\delta^2}{a}\frac{\frac{\pi^2}{3}\left(\frac{b}{a}\right)^2\eta E_x+\left(\frac{\pi^2}{6}-\frac{32}{27}\right)G_{xy}}{\pi^4\left(\frac{b}{a}\right)^2\eta E_x+\left[\frac{\pi^4}{4}-\left(\frac{32}{9}\right)^2\right]G_{xy}},$$

$$C=\frac{\pi^2\delta^2}{b}\frac{\left(\frac{2\pi^2}{3}-\frac{64}{27}\right)\left(\frac{b}{a}\right)^2\eta E_x+\left(\frac{\pi}{6}-\frac{32}{27}\right)G_{xy}}{\pi^4\left(\frac{b}{a}\right)^2\eta E_x+\left[\frac{\pi^4}{4}-\left(\frac{32}{9}\right)^2\right]G_{xy}},$$

$$i=-\frac{\pi^2 D_1 K}{b^2\eta t E_x}-0.755\left(\frac{a}{b}\right)^2\left(\frac{\delta}{b}\right)^2\frac{E_y}{\eta E_x}-\frac{183.6\left(\frac{b}{a}\right)^2\eta E_x+22.4\,G_{xy}}{97\left(\frac{b}{a}\right)^2\eta E_x+11.6\,G_{xy}}\left(\frac{\delta}{a}\right)^2$$
$$-\frac{21.2\left(\frac{b}{a}\right)^2\eta E_x+2.3\,G_{xy}}{97\left(\frac{b}{a}\right)^2\eta E_x+11.6\,G_{xy}}\left(\frac{\delta}{b}\right)^2\frac{G_{xy}}{\eta E_x}$$

and the total applied load is given by

$$P=-\frac{\pi^2 D_1 K}{b}-E_x\eta t b\left\{0.755\left(\frac{a}{b}\right)^2\frac{E_y}{\eta E_x}+\frac{64.4\left(\frac{b}{a}\right)^2\eta E_x+8.1\,G_{xy}}{97\left(\frac{b}{a}\right)^2\eta E_x+11.6\,G_{xy}}\left(\frac{b}{a}\right)^2\right.$$
$$\left.+\frac{21.2\left(\frac{b}{a}\right)^2\eta E_x+2.3\,G_{xy}}{97\left(\frac{b}{a}\right)^2\eta E_x+11.6\,G_{xy}}\frac{G_{xy}}{\eta E_x}\right\}\frac{\delta^2}{b^2}. \tag{23b}$$

d) Zero Edge Transverse Stress (Stiffened Flat Plate). The previous result, Eq. (23b), has been derived on the basis of a corrugated plate for which the transverse membrane stress along the unloaded edge is presumed to be zero. For a stiffened flat plate, however, $E_x=E_y=E$, $G_{xy}=\frac{E}{2(1+\mu)}$, $\mu=0.3$ and Eq. (23b) can be rewritten as

$$P=-\frac{\pi^2 D_1 K}{b}-E\,\eta\,t\,b\left(\frac{\delta}{b}\right)^2\left\{\frac{0.755}{\eta}\left(\frac{a}{b}\right)^2+\frac{1}{97\left(\frac{b}{a}\right)^2\eta+4.25}\left[64.4\left(\frac{b}{a}\right)^4\eta\right.\right.$$
$$\left.\left.+3.04\left(\frac{b}{a}\right)^2+\frac{1}{\eta}7.96\left(\frac{b}{a}\right)^2+\frac{1}{\eta}0.325\right]\right\}. \tag{24}$$

Plastic Post-buckling

1. Introduction

The mechanism shown in Fig. 4 is assumed to form within a long, plane plate after the ultimate load is reached. In a rigid-plastic theory, the plate is assumed to remain plane prior to the attainment of the ultimate load. The hinge pattern proposed consists of flat planes rotating about particular axes, some flats moving outward and others inward. All the hinge lines are assumed

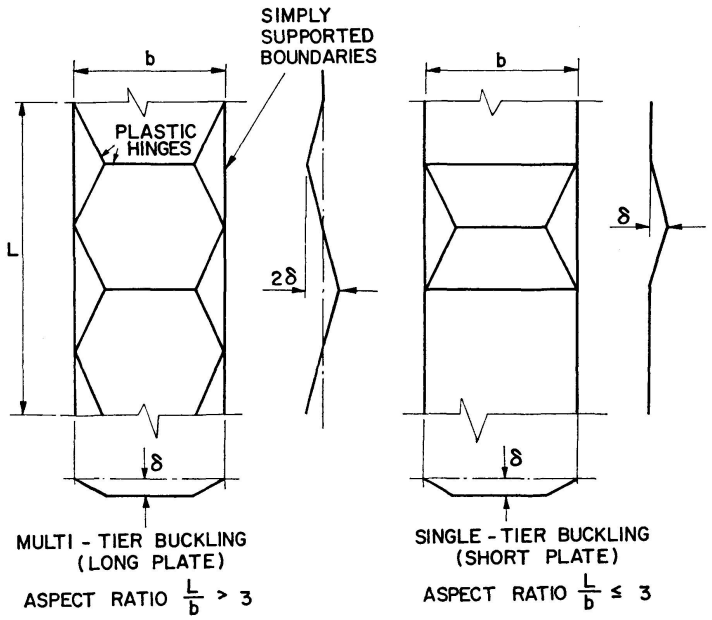

Fig. 4. Plastic Mechanisms.

to remain straight and triangular segments rotate about their edges. As soon as the mechanism is formed within the plate the applied load will decrease with increasing deflexion. It has been assumed that the wave length of a plastically buckled plate has the same value as the wavelength in elastic buckling; because of the development of membrane stresses, however, the longitudinal half wavelength become smaller with increases in lateral deflexion.

Owing to the relative rigidities for the two directions of the stiffened plate, analytical arguments suggest that the triangular areas adjacent to the unloaded edges become very narrow. It follows, then, that a mechanism pattern can be assumed as shown in Fig. 5 and the lateral deflexion of a typical horizontal yield line is a function of the form, $\delta \cos \frac{\pi y}{b}$. The transverse membrane stress has the distribution shown which is also a cosine function in the transverse direction. The normal component (z direction) of the transverse membrane stress is assumed to be specified by

$$f = T^0\left(1 - \frac{4x}{a}\right) \cos \frac{\pi y}{b} \frac{\partial^2 \omega}{\partial y^2},$$

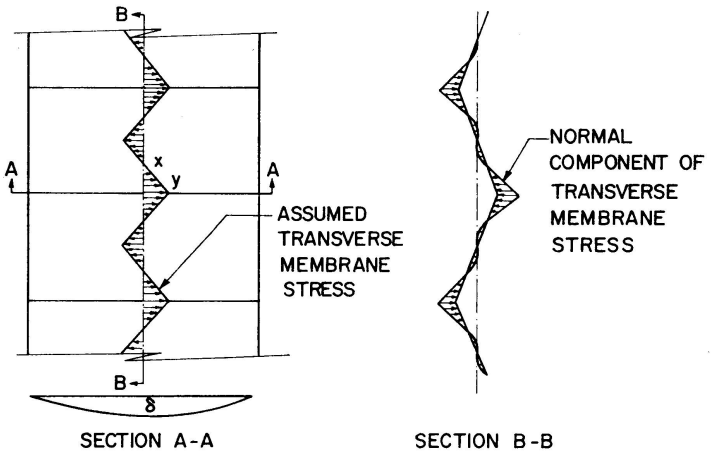

Fig. 5. Mechanism for Long Stiffened Plate.

where T^0 is the transverse membrane force intensity at $x=0$, $y=0$, and the deflexion ω is assumed to be

$$\omega = \delta\left(1-\frac{2x}{a}\right)\cos\frac{\pi y}{b}.$$

2. *The Corrugated Section*

The buckled plate is treated as an aggregation of strips in the x-direction, having a cross-section as indicated in Fig. 6. Each strip is treated as an equivalent column which buckles into the shape shown in Fig. 6b. Considering one part of this strip, AB, one finds that, in addition to the plastic moment, M_0 and applied load P, there is a distribution of lateral load along AB which is actually the normal component, f, of the membrane stress given by

$$f = -T^0\delta\left(1-\frac{2x}{a}\right)\left(1-\frac{4x}{a}\right)\left(\frac{\pi}{b}\right)^2\left(\cos\frac{\pi y}{b}\right)^2. \tag{25}$$

The membrane stress at $x=0$, $y=0$, can be found by considering the cross-section of the central corrugation, where, at large deflection, plastic moments occur at the fold (ridge) due to tension (Fig. 3a) such that

$$M_0 = F\frac{d}{2} = T^0\frac{d}{2}.$$

For a section of thickness t under tension, $T^0\cos\phi = T_0/\eta$, the plastic moment is:

$$M_0 = \frac{\sigma_0}{4}\left[t^2-\left(\frac{T^0}{\sigma_0\eta}\right)^2\right]$$

and

$$T^0 = \sigma_0\eta^2 d\left[-1+\sqrt{1+\left(\frac{t}{\eta d}\right)^2}\right], \tag{26}$$

where σ_0 is the yield stress of the material. Fig. 6a shows the cross-section of a strip. If A_1 is the area in compression and A_2 is the area in tension, then the net area for a single strip

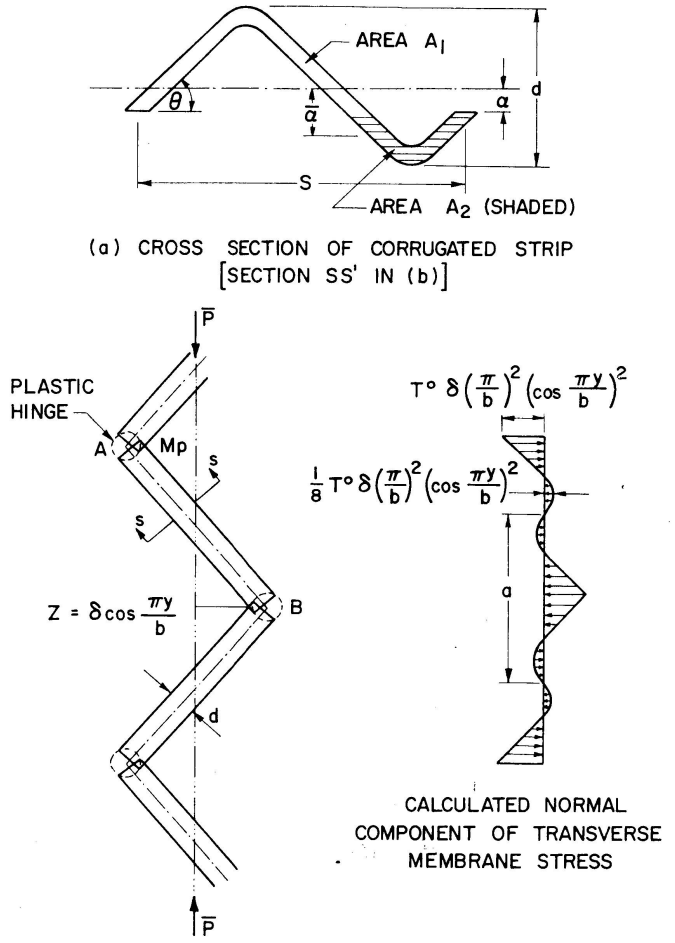

Fig. 6. Buckled Shape and Membrane Action in Corrugated Strip.

$$\bar{A} = A_1 - A_2$$

and $A_1 - A_2 = 2\frac{2\alpha}{\sin\phi}t$ where α is the distance shown. Letting $\frac{2}{\sin\phi}t = \bar{t}$ the applied load on this strip is

$$\bar{P} = \sigma_0 (A_1 - A_2) = 2\bar{t}\,\alpha\,\sigma_0 \quad \text{or} \quad \alpha = \frac{\bar{P}}{2\bar{t}\,\sigma_0}. \tag{27}$$

The limit moment becomes

$$M_0 = 2A_2\bar{\alpha}\,\sigma_0 = 2A_2\frac{\frac{d}{2}+\alpha}{2}\sigma_0 = \frac{1}{2}(A^* - 2\bar{t}\,\alpha)\left(\frac{d}{2}+\alpha\right)\sigma_0,$$

where $A^* = A_1 + A_2$ is the total cross-sectional area of the strip. Substituting (27) into the above expression

$$M_0 = \frac{A^* d}{4}\sigma_0 + (A^* - \bar{t}\,d)\frac{\bar{P}}{4\bar{t}} - \frac{\bar{P}^2}{4\bar{t}\,\sigma_0}$$

and since $A^* \cong \bar{t}\,d$

$$M_0 \cong \frac{A^* d}{4}\sigma_0 - \frac{\bar{P}^2}{4\bar{t}\,\sigma_0}. \tag{28}$$

From the condition of moment equilibrium of strip $A\,B$.

$$\bar{P}z = M_0 + s\frac{a}{2}\int_0^{a/2} f\,dx - s\int_0^{a/2} f\,x\,dx.$$

Substituting Eq. (25) into the above

$$\bar{P}z = M_0 + \frac{a^2 s}{24} T^0 \delta \left(\frac{\pi}{d}\right)^2 \left(\cos\frac{\pi y}{b}\right)^2.$$

Using expression (28), this equation can be rewritten as

$$\left(\frac{\bar{P}z}{A^*\sigma_0}\right)^2 + 4\left(\frac{z}{b}\right)\left(\frac{b}{d}\right)\left(\frac{\bar{p}}{A^*\sigma_0}\right) - 1 - \frac{a^2 s}{6A^* d\sigma_0} T^0 \delta \left(\frac{\pi}{b}\right)^2 \left(\cos\frac{\pi y}{b}\right)^2 = 0,$$

since $A^* = \eta s t$, $z = \delta \cos\frac{\pi y}{b}$ and setting $\frac{\bar{P}}{A^*\sigma_0} = \bar{p}$

$$\bar{p}^2 + 4\left(\frac{b}{d}\right)\left(\frac{\delta}{b}\right)\bar{p}\cos\frac{\pi y}{b} - 1 - \frac{\pi^2}{6\eta t d\sigma_0} T^0 \delta \left(\frac{a}{b}\right)^2 \left(\cos\frac{\pi y}{b}\right)^2 = 0$$

and substituting (26) into this equation

$$\begin{aligned}\bar{p}^2 + 4\left(\frac{b}{d}\right)\left(\frac{\delta}{b}\right)\bar{p}\cos\frac{\pi y}{b} - 1 \\ - \frac{\pi^2}{6}\eta\left(\frac{d}{t}\right)\left(\frac{\delta}{b}\right)\left(\frac{b}{d}\right)\left[-1 + \sqrt{1 + \left(\frac{t}{\eta d}\right)^2}\right]\left(\frac{a}{b}\right)^2\left(\cos\frac{\pi y}{b}\right)^2 = 0.\end{aligned} \tag{29}$$

Substitute $\delta^* = -\frac{\pi^2}{6}\eta\left(\frac{d}{t}\right)\left(\frac{\delta}{b}\right)\left(\frac{b}{d}\right)\left[-1 + \sqrt{1 + \left(\frac{t}{\eta d}\right)^2}\right]\left(\frac{a}{b}\right)^2\left(\cos\frac{\pi y}{b}\right)^2$,

then $\bar{p} = -2\left(\frac{b}{d}\right)\left(\frac{\delta}{b}\right)\cos\frac{\pi y}{b} + \sqrt{1 - \delta^* + \left[2\left(\frac{b}{d}\right)\left(\frac{\delta}{b}\right)\cos\frac{\pi y}{b}\right]^2}$,

where δ^* is a modification factor of the plastic buckling equation for the column.

The total applied load on the plate is given by

$$P = \sigma_0 \eta b t \int_{-b/2}^{b/2} \bar{p}\,dy. \tag{30}$$

On substituting the values of η, a, b, d, t in Eqs. (29) and (30), a relationship is obtained between P and δ/b, which is the plastic post-buckling unloading line. This equation is expressed in non-dimensional form and the parameters $\frac{P}{P_0} = \frac{P}{\sigma_0 A}$ and $\Delta = \frac{\delta}{b}$ are used.

3. The Stiffened Flat Plate

A cross-section at a hinge line of the stiffened flat plate is shown in Fig. 7. A tension area is assumed to develop from the end of the stiffener (shown cross-hatched). $A\,A'$ is the neutral axis dividing compression and tension areas.

In this case, when the stiffeners are equal angles, of thickness equal to the plane plate, the total applied load over this section is

$$\bar{P} = \sigma_0 t (s + 2x).$$

The resisting moment of the hinge section becomes

$$M_0 = \sigma_0 t \left\{ s t + \frac{d^2}{2} - \frac{1}{4}\left(\frac{\bar{P}}{\sigma_0 t} - s\right)^2 \right\}$$

and using a moment equilibrium equation similar to that used previously, obtain the load-deflexion relationship

$$\left(\frac{\bar{P}}{\sigma_0 t} - s\right)^2 + 4\left(\frac{\bar{P}}{\sigma_0 t} - s\right) z - 4\left\{ s(t-z) + \frac{d^2}{2} + \frac{\pi^2}{24}\left(\frac{a}{b}\right)^2 \frac{T^0 s}{\sigma_0 t}\delta\left(\cos\frac{\pi y}{b}\right)^2 \right\} = 0. \quad (31)$$

This equation is not applicable after AA' reaches the corner of the stiffener, i.e., $x \leqq t$. For this case, the resisting moment can be considered to be taken by the stiffener only.

$$M_0' = \sigma_0 \frac{t d^2}{2}$$

and the equilibrium equation reduces to

$$P' z = \sigma_0 \frac{t d^2}{2} + \frac{a^2 s}{24} T^0 \delta \left(\frac{\pi}{b}\right)^2 \left(\cos\frac{\pi y}{b}\right)^2. \quad (32)$$

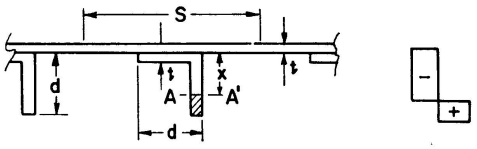

Fig. 7. Section of Stiffened Plate.

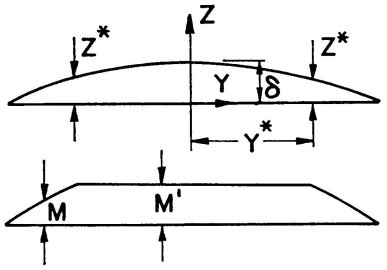

Fig. 8. Moment Distribution Across the Stiffened Plate.

The load is taken by the flat plate portion of the section and the stress will be less than the yield stress, i.e., $\bar{P}' = S t \sigma_e$ where σ_e is the elastic stress. When $x = t$

$$S t \sigma_0 z^* = M_0' \quad \text{or} \quad z^* = \frac{d^2}{2S}.$$

Therefore, when the deflexion of this section is less than Z^*, the load-deflexion relation will be given by Eq. (31). For $x < t$, the appropriate load deflexion relation is given by Eq. (32). Fig. 8 gives the moment distribution across the

plate. The total applied load on the plate is

$$P = 2\int_0^{y^*} \frac{\bar{P}'}{s}\,dy + 2\int_{y^*}^{b/2} \frac{\bar{P}}{s}\,dy,$$

where $\bar{P}$ and $\bar{P}'$ are given by Eqs. (31) and (32).

Experimental

1. Corrugated Cylinders

Tubes of square cross-section (Fig. 9) were tested under uniform edge compression to determine the behaviour of a simply supported plate subjected to inplane compression. The tubes were fabricated from 575-H 34 aluminum alloy with a tensile stress-strain relationship shown in Fig. 10. The yield stress obtained from a 0.2% strain offset was taken to be 32.0 ksi.

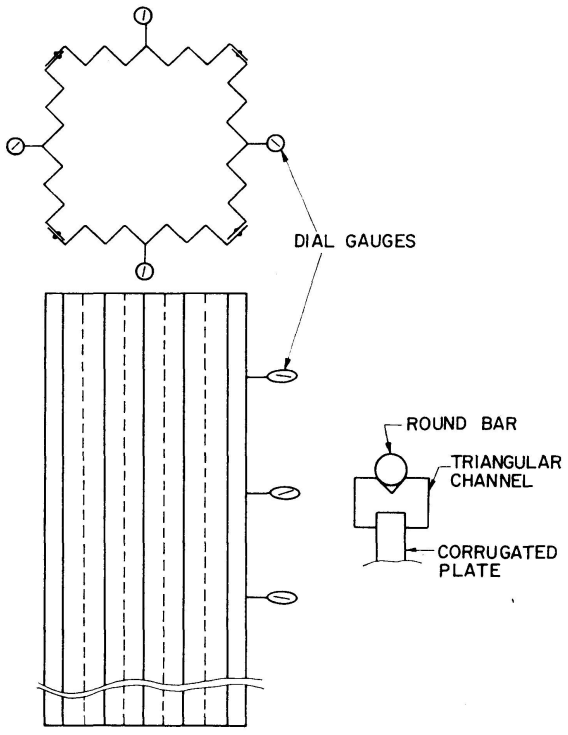

Fig. 9. Tube with Corrugated Walls.

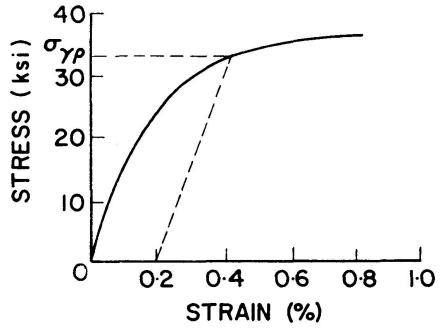

Fig. 10. Stress-Strain Relationship 575-H 34 Aluminum Alloy.

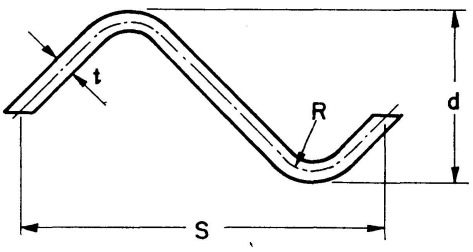

Fig. 11. Cross-Section of Corrugation.

Two different cross-sections of corrugation were used (Fig. 11) and Table 1 gives the properties of these two cross-sections. Seven tubes with cross-section I and four tubes with cross-section II were fabricated from corrugated sheets. Small tolerances on the dimensions were specified to ensure uniform loading on the horizontal edges during testing.

Table 1. Details of Corrugated Test Specimens

Corrugated Cross-Section I	*Corrugated Cross-Section II*
t = 0.067 in.	0.032 in.
s = 0.906 in.	0.488 in.
d = 0.407 in.	0.220 in.
R = 0.112 in.	0.100 in.
Area/unit width = 0.087 in²/in	0.040 in²/in
I_x/unit width = 11.25×10^{-4} in⁴/in	1.56×10^{-4} in⁴/in
Radius of Gyration = 0.114 in.	0.0625 in.
I_y/unit width = 0.213×10^{-4} in⁴/in	0.025×10^{-4}/in⁴/in

In order to ensure hinged boundary conditions at the loaded ends, round bars and triangular channels were used to distribute the load in all the type I tubes. A comparison between the analytical and the experimental results did not produce good correlation for short tubes. This is attributed to the triangular channels which did not produce a satisfactory edge condition. On the other hand, the long tubes, whose sides buckled into more than two half waves showed a closer correlation between test and theory. The conclusion to be drawn from this result is that the simply supported boundary condition may be obtained by considering a one half wavelength of a long sheet as a simply supported plate. In all the tests performed, the loads were applied by a 200^k Riehle Screw Gear Machine possessing two rigid flat platens. The resulting buckling pattern supported the view that the load was applied uniformly along the tube edges.

Four dial gauges were placed on each of the four sheets of a tube to measure the lateral deflexion of the centre line, i.e., x-axis. If the plates of the tube buckled into one half wave, as they did for a single case, the maximum deflexion

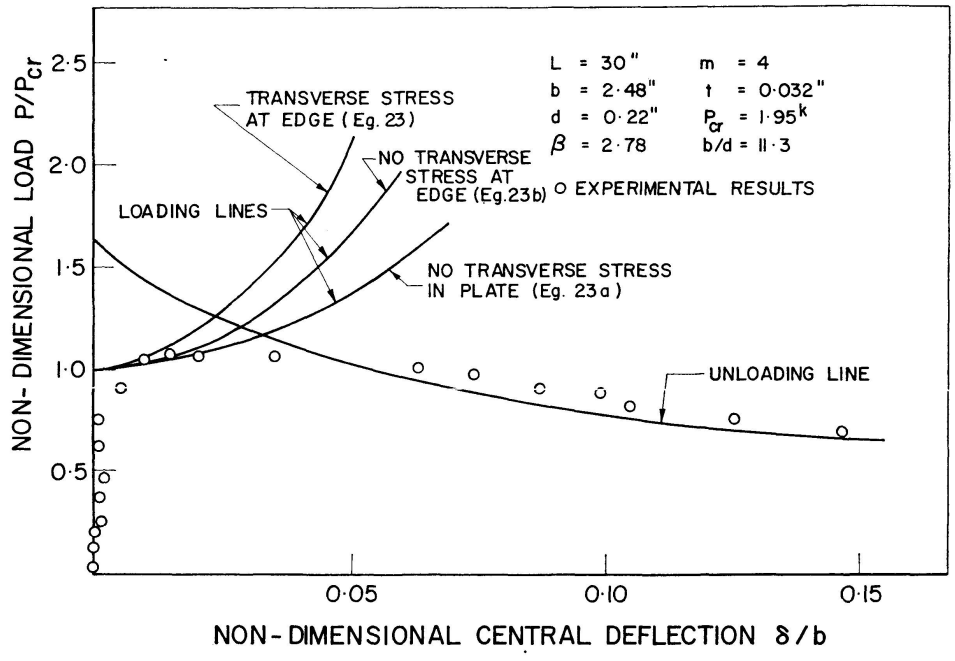

Fig. 12. Load-Deflexion Behaviour of the Corrugated Plate (Type II).

was found by assuming that the buckled shape was a cosine curve. For other tests, in which there was more than one half wave as many dial gauges were moved to the positions of maximum deflexion as half-waves at the time they were noticed.

In Figs. 12 to 19, the experimental results together with the theoretical elastic (Eqs. (23), (23a) and (23b)) and plastic (Eq. (30)) post-buckling curves

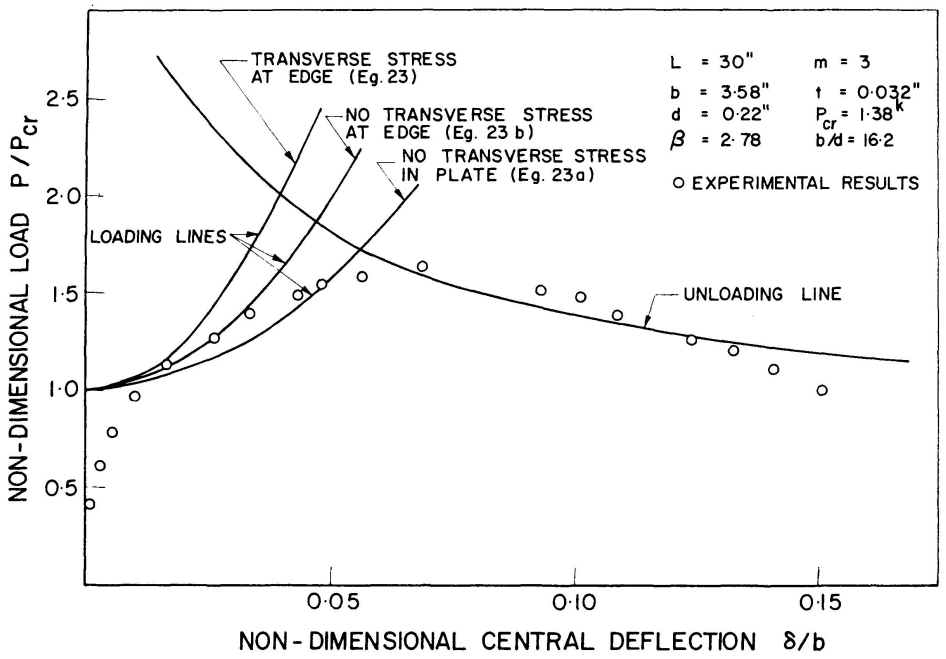

Fig. 13. Load-Deflexion Behaviour of the Corrugated Plate (Type II).

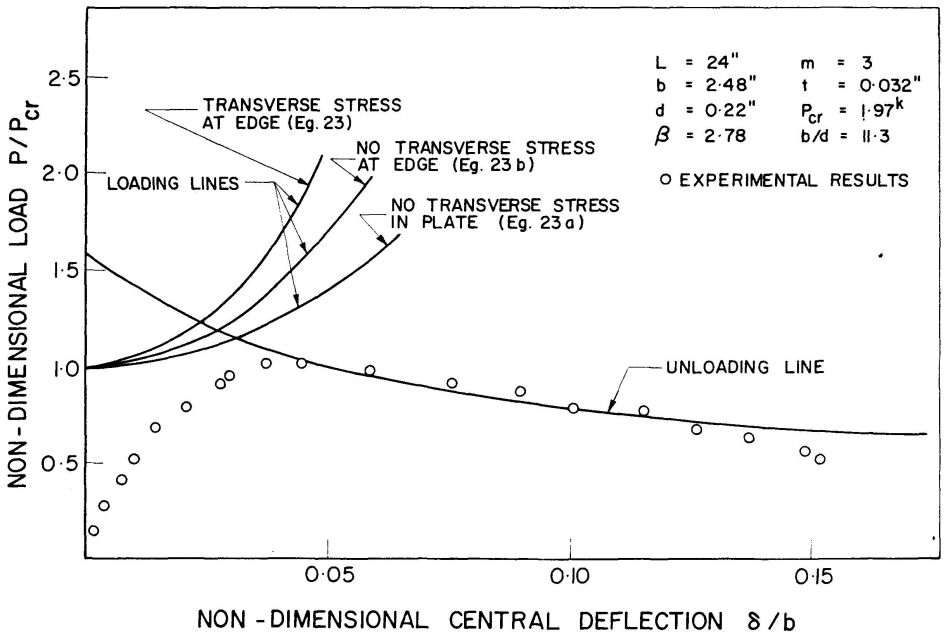

Fig. 14. Load-Deflexion Behaviour of the Corrugated Plate (Type II).

were plotted on load-deflexion diagrams. The elastic post-buckling curves represent three cases:

1. Eq. (23) – using the value of E_y derived, this equation is based on the assumption that the plate has straight supported edges and a variation in membrane stress along the edges.

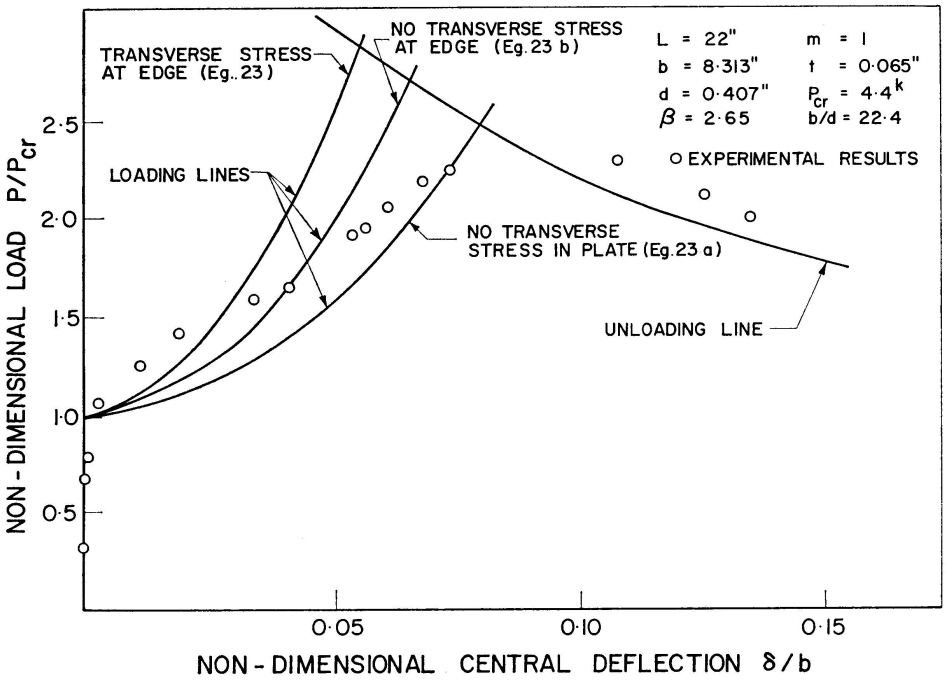

Fig. 15. Load-Deflexion Behaviour of the Corrugated Plate (Type I).

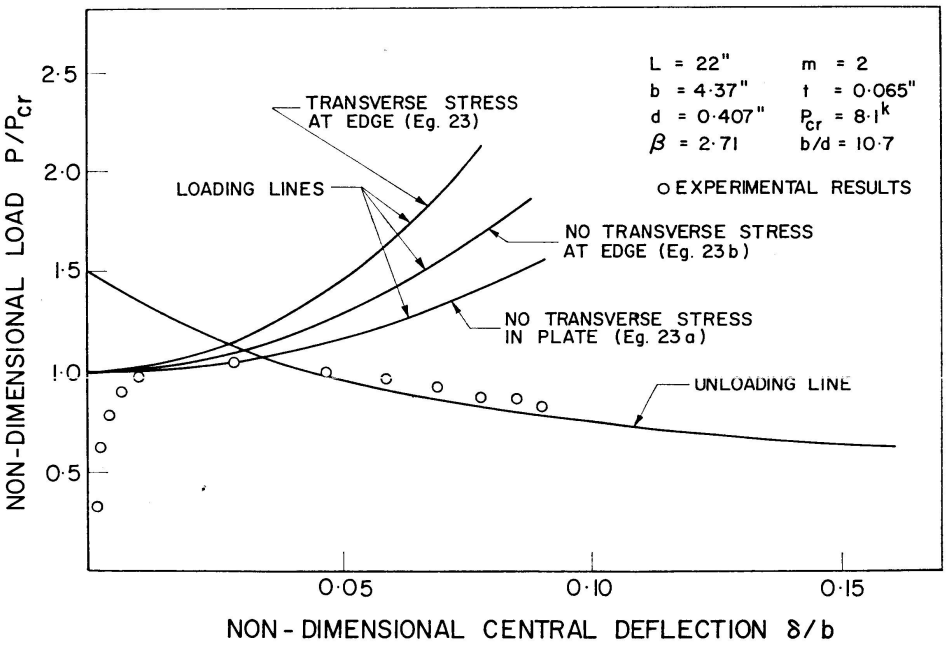

Fig. 16. Load-Deflexion Behaviour of the Corrugated Plate (Type I).

2. Eq. (23a) – no transverse membrane stress exists in corrugated plates.
3. Eq. (23b) – edges are straight and free of transverse stress.

It is found that Eq. (23b) gives the best agreement between theory and experiment. In the case of short plates, $m < 3$, the experimental results gave a higher value of load than the theoretical upper bound for the elastic loading path as obtained by Eq. (23b). This apparent paradox is due to the short tubes not satisfying the simply supported boundary condition at the loaded

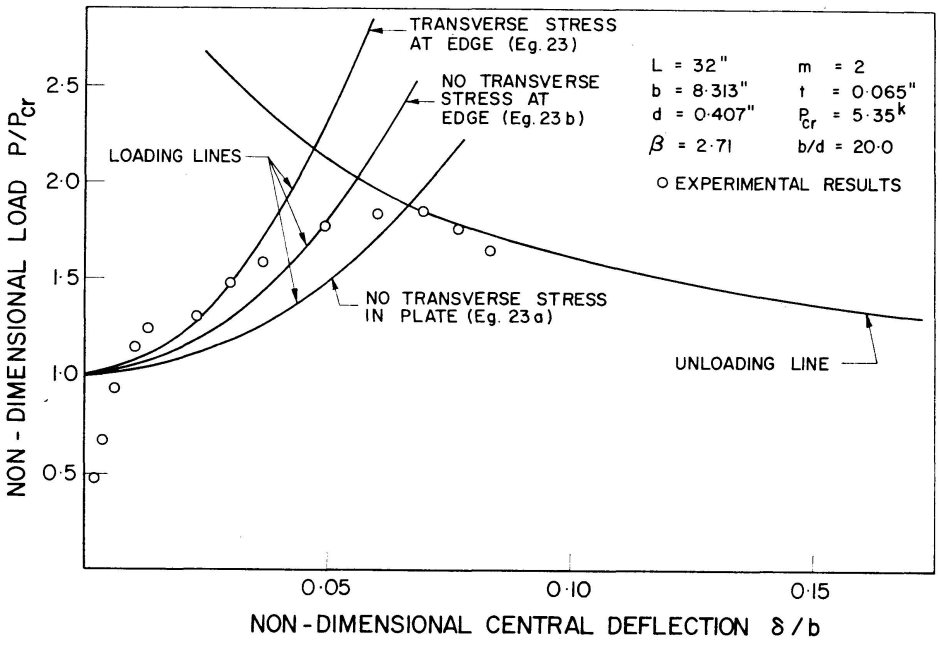

Fig. 17. Load-Deflexion Behaviour of the Corrugated Plate (Type I).

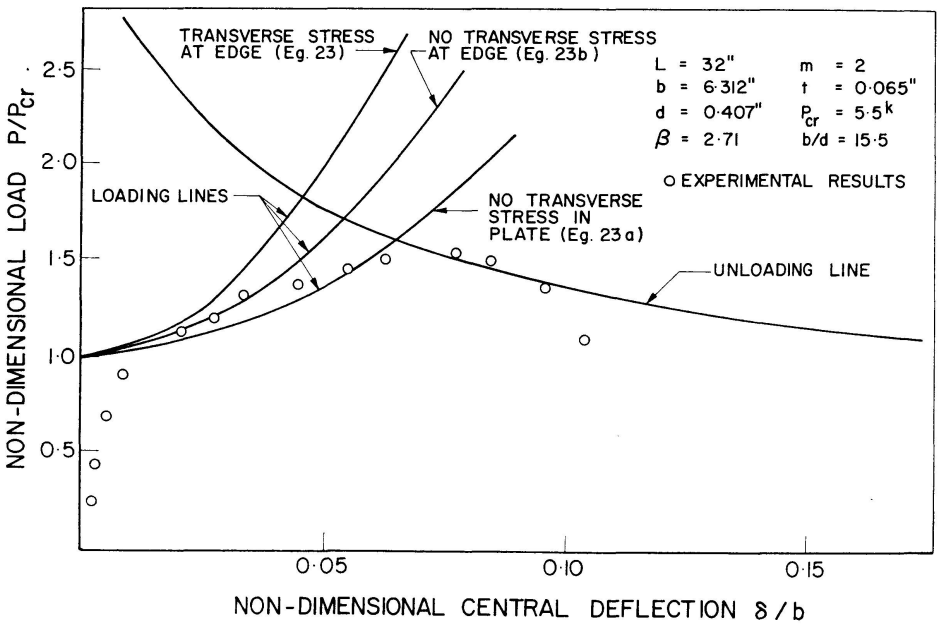

Fig. 18. Load-Deflexion Behaviour of the Corrugated Plate (Type I).

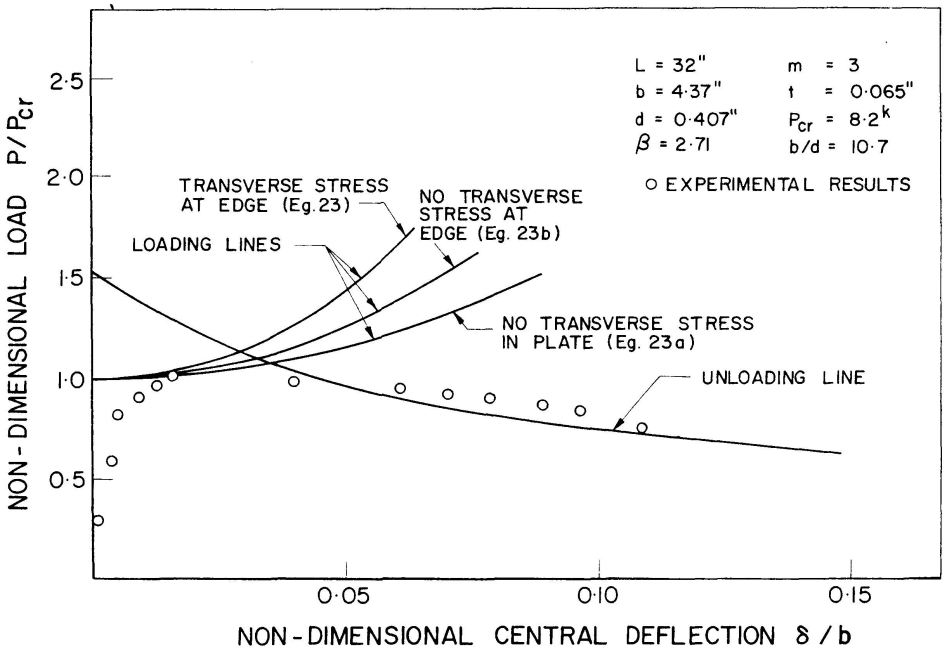

Fig. 19. Load-Deflexion Behaviour of the Corrugated Plate (Type I).

edges. For these cases, there was only one half-wave formed and the condition at the loaded edges was partly fixed, rather than simply supported, leading to a higher critical load. For the remaining tubes, i.e., where more than two half-waves formed, the simply supported edge condition was closely approximated and hence good agreement with theory was obtained.

For the plastic-post-buckling curves shown, it is observed that, for the same load, experimental results give slightly larger deflexion than those obtained theoretically.

2. Corrugated Plate

A $30'' \times 2.48''$ tube, with thirty-four strain gauges attached to one of its four sheets, was tested. The strain gauges were distributed in a region as shown in Fig. 20, which was presumed to be one of the largest lateral deflexions. Gauges were also placed along one edge of a given sheet near a supported edge, five on each of the inside and outside faces; these gauges were oriented to determine the transverse membrane stress along the supported edge. Ten gauges were positioned along the centre line of the plate, $y=0$, five on each face, inside and outside, of the sheet; these were used to measure the longitudinal strain. Six additional gauges, three on each face, were located across the plate to determine the longitudinal stress along the y axis.

In considering the longitudinal stress of a corrugated plate, the longitudinal strain due to the transverse membrane stress is small, hence the effect of transverse membrane stress will be neglected. Under this assumption, the longitudinal stress can be determined from the strain in that direction by employing

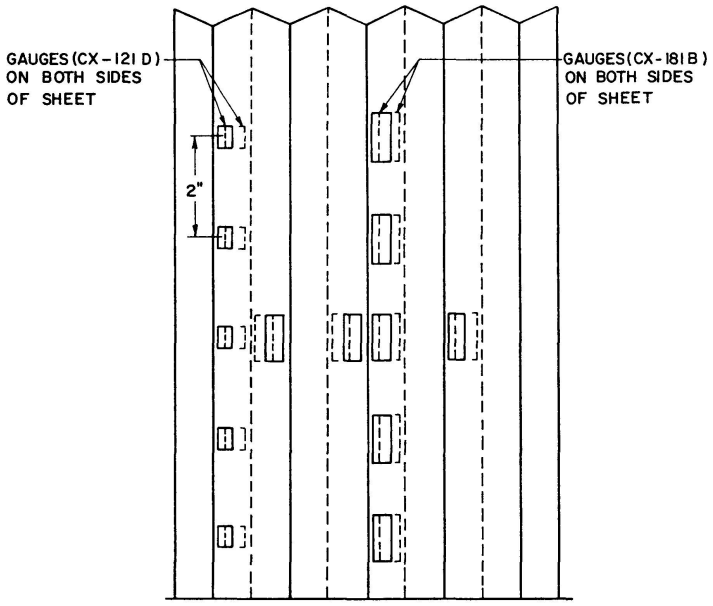

Fig. 20. Distribution of Strain Gauges.

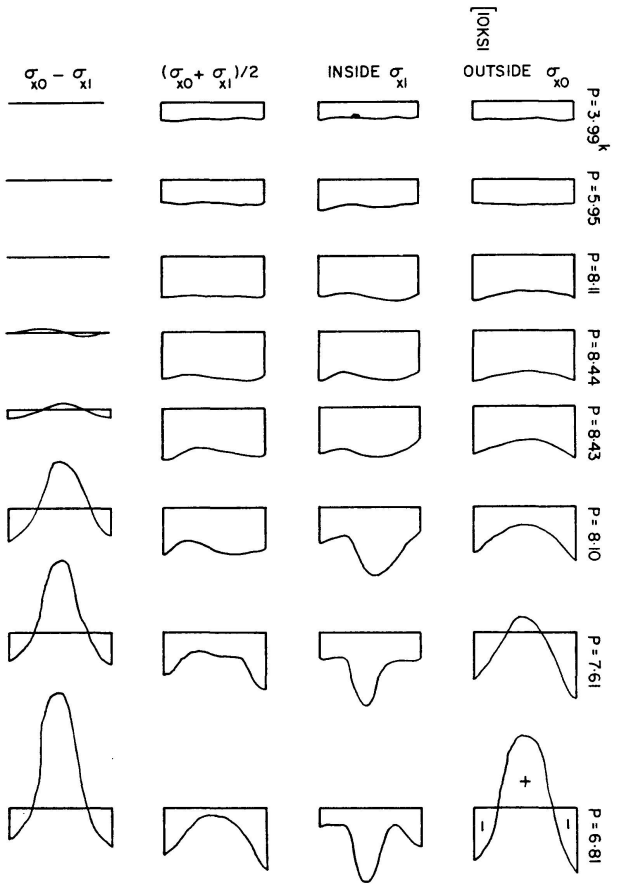

Fig. 21. Variation of Longitudinal Stress along the x-Axis at $y=0$.

the known stress-strain relationship of the material. On the other hand, in considering the transverse membrane strain, the longitudinal stress is significant. From Hooke's law and taking Poisson's ratio $\mu=0.3$, the transverse membrane stress can be obtained as

$$\sigma_y = \frac{E}{1-\mu^2}(\epsilon_y + \mu\,\epsilon_x),$$

where ϵ_y is the transverse strain and ϵ_x is the longitudinal strain.

It must be emphasized that Figs. 21 and 22 show the distribution of stress in a region (8 inches in the longitudinal direction) which is longer than the actual length of a half-wave. The theoretical half-wave length at elastic

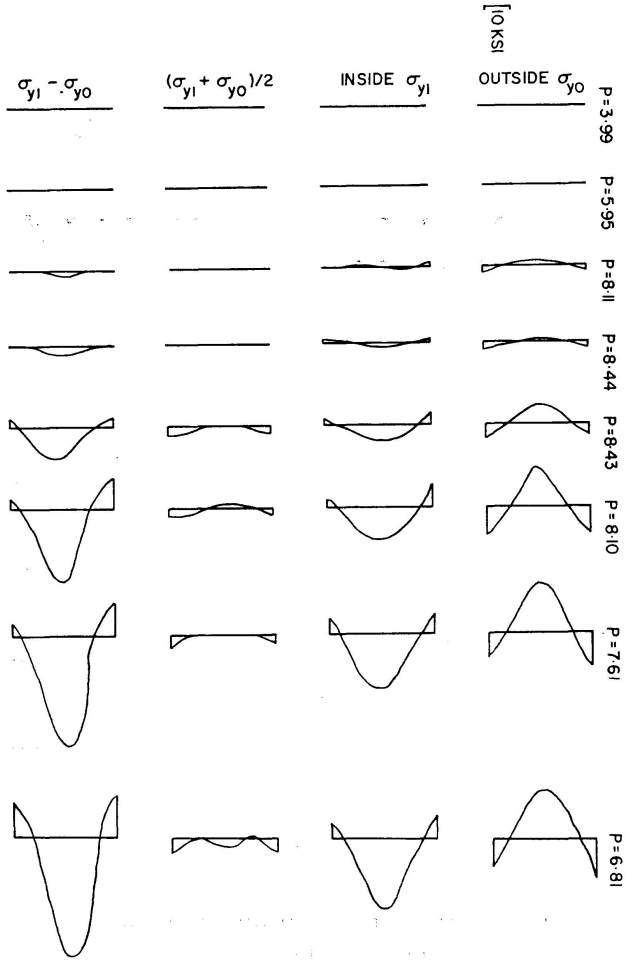

Fig. 22. Variation of Transverse Membrane Stress along the Edge ($y = \pm b/2$).

buckling was found to be equal to 6.85 inches for this case. Furthermore, as indicated in Appendix II, an approximate formula is derived showing that the buckled length shortens under increasing load and deflexion. For example, at $P = 6.81^k$, $\frac{\delta}{b} = 0.125$ and $K = \frac{\beta}{1.22}$, the half-wavelength decreasing to 5.65 inches.

The experimental transverse membrane stresses, i.e., the average values in Fig. 22, were found to be very small along the supported edge. Hence the assumption that there are negligible membrane stresses along the supported edges is shown to be reasonable. With the values of stress on both faces of the plate, the approximate distributions of stress across the section in either transverse or longitudinal directions can be plotted as shown in Fig. 23, and the

moments can easily be calculated. In Figs. 24, 21 and 22, the last entries of the patterns shown (i.e., $\sigma_I - \sigma_0$ or $\sigma_0 - \sigma_I$) represent only a measure of the variation of bending moment. These stress differences are not proportional to each other in corresponding figures. The variations of moment in the longitudinal direction (Figs. 24 and 21) show good agreement with the theory. In the transverse direction, however, the moments do not agree with the assump-

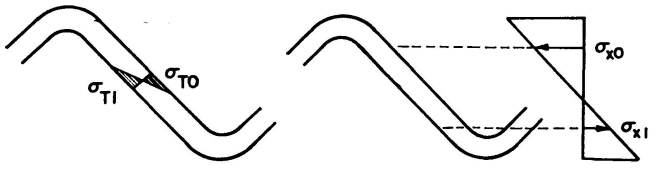

(a) DISTRIBUTION OF TRANSVERSE MEMBRANE STRESS

(b) DISTRIBUTION OF LONGITUDINAL STRESS

Fig. 23. Stresses in Corrugation.

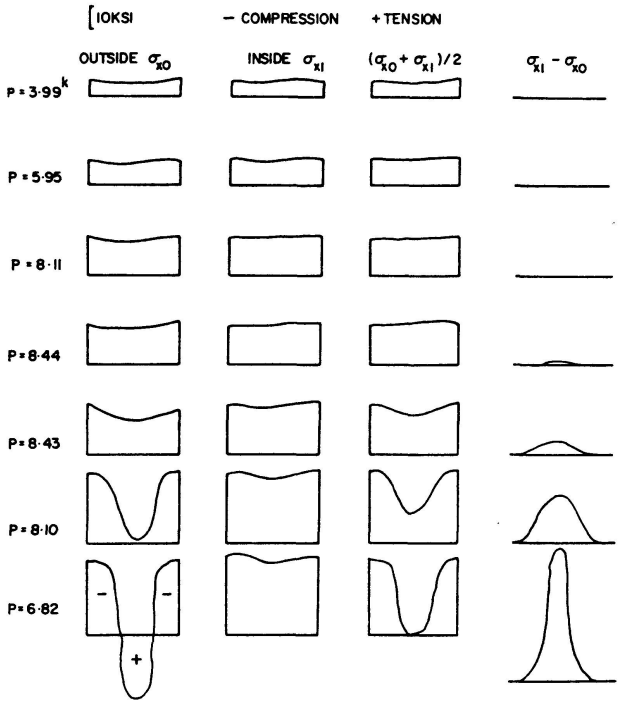

Fig. 24. Variation of Longitudinal Stress along y axis and $x=0$.

tion of a simply supported edge. This is caused by edge restraint which arises from twist at the edge. The value of this resisting moment is small in comparison with the moment in the longitudinal direction. For example, in the transverse direction, at $P=6.81^k$, $\sigma_{yI}=45.0$ ksi, the maximum amount of twist at the edge is equal to 3.6×10^{-3} lb in/in, while, for a stress difference $\sigma_{x0}-\sigma_{xI}=48$ ksi the maximum longitudinal moment is 4.5×10^{-1} lb in/in.

3. Stiffened Flat Tube

A stiffened flat tube, with dimensions $30''\times7.5''\times7.5''$, was tested under axial compression; the load was applied by a hydraulic jack. Along the loaded

edges, the ends of the stiffeners were trimmed at an angle of 45° to ensure the simply supported edge-condition. The stiffeners were 5/16″×5/16″ angles, with a spacing of 1.5″. Fig. 25 shows the cross-section of this tube.

The plate and stiffeners had the same thickness, namely 0.032″. Upon loading, the sheets buckled into a one half-wave configuration. Soon afterwards the tube failed, local buckling occurring at the corner before the ultimate load was reached. Hence, the results represent essentially only elastic behaviour as given in Fig. 26.

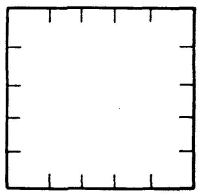

Fig. 25. Cross-Section of Stiffened Tube.

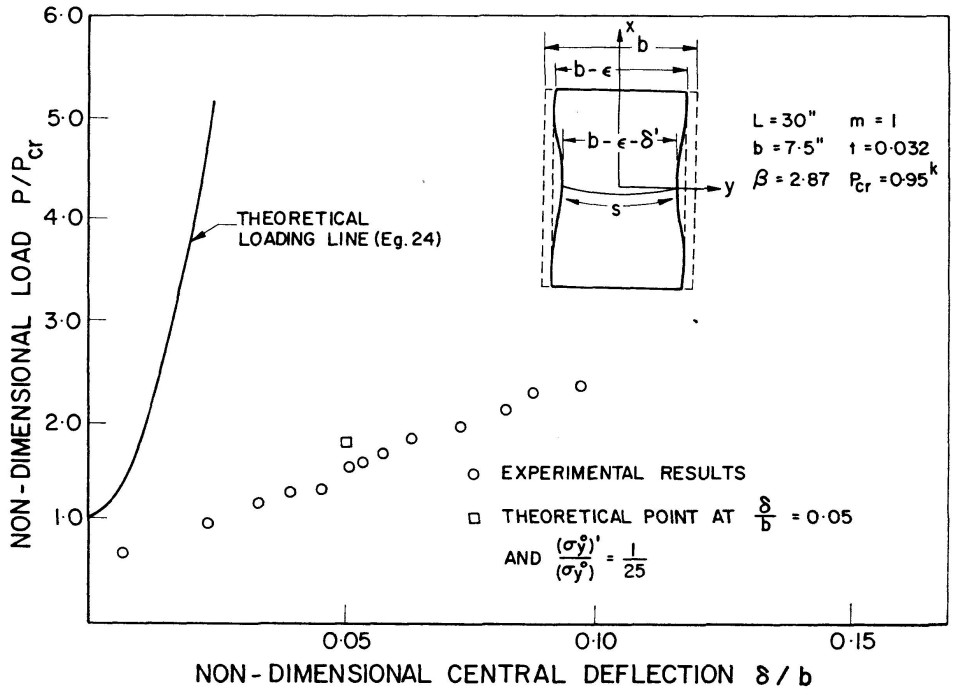

Fig. 26. Load-Deflexion Behaviour of Stiffened Plate.

The experimental results for this tube in elastic, post-buckling are shown to be in sharp disagreement with Eq. (24). This result may be attributed to the corners of the stiffened tube not remaining straight under loading. When this occurs, the membrane stress, $(\sigma_y^0)'$ can be easily found by assuming a relative shortening δ' (Fig. 26). The following relationship for the transverse shortening of the mid-plane can be derived

$$S-(b-\epsilon-\delta') = \frac{1}{2}\int_{-b/2}^{b/2}\left(\frac{\partial \omega}{\partial y}\right)_{x=0} dy = \left(\frac{\pi}{b}\right)^2 \frac{\delta^2 b}{4},$$

where S and ϵ have been defined previously. After substituting the values of S and ϵ, obtain

$$\frac{(\sigma_y^0)'}{(\sigma_y^0)} = 1 - \frac{4}{\pi^2}\left(\frac{b}{\delta}\right)^2 \frac{\delta'}{b},$$

where $(\sigma_y^0) = \frac{\pi^3}{16} E_y \left(\frac{\delta}{b}\right)^2$, is the membrane stress with straight edges. Hence if δ is measured in the test, the corresponding membrane stress can be estimated. For example, if $\frac{\delta'}{b} = 0.006$ and $\frac{\delta}{b} = 0.05$ then

$$\frac{(\sigma_y^0)'}{(\sigma_y^0)} = \frac{1}{25}.$$

The actual shortening could have been measured but, in this test, no such information was recorded. Fig. 26 gives the test results and the theoretical results for the straight edge-condition. The square (as shown) is computed at $\frac{\delta}{b} = 0.05$, assuming $\frac{\delta'}{b} = 0.006$, i.e., $\delta = 0.045''$.

Conclusions

The buckling and post-buckling behaviour of a plate with two different orthogonal rigidities has been investigated. Corrugated and stiffened flat plates have been used to represent this type of structural element. In the case of long corrugated plates, the critical loads have been shown to reflect good agreement between theoretical and experimental results. In the case of short tubes, the critical loads have been underestimates, since the existence of a resisting moment at the loaded edges prevented the simply supported edge condition from being realised.

Three different distributions of transverse membrane stress in corrugated plates have been assumed. The experimental results show best agreement for the case of zero transverse membrane stress along the supported edges.

The compressive stress along the loaded edges was assumed to be uniform and the supported edges assumed to remain straight in the theoretical analysis. Strictly speaking, however, this is not true due to mid-plane deflexions. Furthermore, the experiments on box sections show that the supported edges do not remain straight under loading. The deformations of the edges will be small in a tube of corrugated sheets due to the rigidity; the deformations are significant in a tube of stiffened flat plates.

It is noticed from the test results that plates with large values of $\frac{b}{d}$, i.e., with small corrugations, have significant elastic postbuckling strengths compared to those with small $\frac{b}{d}$.

Generally speaking, good agreement has been obtained with corrugated plates when the behaviour is elastic. The experimental results for plastic

unloading are somewhat higher than the theoretical curves. In the test of a stiffened tube, the theory failed to give a good description of the elastic post-buckling behaviour because of deformed edges and eccentricity of loading.

The phenomenon of changing wavelength, after buckling, was not considered in the main text. A discussion is given in Appendix II.

The following suggestions are made for further tests:

1. The minimum length of tube should be at least three times the length of the elastic buckling half-wave.
2. Sections with small corrugations ($\frac{b}{d} > 15$), should be employed.
3. The deformation of edges should be measured in tests to define the actual boundary conditions.
4. A symmetric section of a stiffened flat plate which has stiffeners on both sides is suggested.
5. Tubes fabricated from continuous sheet are suggested as opposed to those made from four independent sheets joined by rivets as reported here.

Acknowledgments

This work was carried out in the Department of Civil Engineering of the University of Waterloo under National Research Council of Canada Grant No. A-1582 and with funds supplied by Alcan Limited.

Appendix I

Notation

The following symbols were used throughout this paper:

a	half wavelength of buckling
b	width of plate
d	depth of corrugated cross-section
E	elastic modulus
E_x, E_y	elastic moduli in x and y directions
f	normal component of transverse membrane stress
I_x, I_y	moments of inertia in x and y directions
L, l	length of plate
A, A^*	area of plate cross-section; cross-sectional area of single strip
M_0	plastic moment of hinge section
m	number of half-waves
P	total applied load
P_0	squash load
$\bar{P}$	applied load on a strip of plate

$\bar{p}$	nondimensional applied load $\bar{P}/A^* \sigma_0$
S	length of post-buckling curve at mid-plate ($x=0$) in transverse direction
s	net width of single corrugation
T, F	transverse membrane force per unit length, width
T^0	transverse membrane force intensity at origin (0,0)
t	true thickness
$t', \bar{t}$	equivalent thicknesses
u, v	the displacement of mid-plane in x and y directions
w	deflexion at (x, y)
z	deflexion along y axis ($x=0$)
δ	deflexion at centre of plate
Δ	nondimensional deflexion δ/b
η	nondimensional thickness $= t'/t = A/bt$
μ	Poisson ratio
μ_x, μ_y	directional values of Poisson's Ratio
ϵ	shortening of plate in transverse direction
σ_x, σ_y	stresses at (x, y) in x and y directions
σ_y^0, σ_x^0	stresses at origin (0,0) in x and y direction
$\sigma_{x\mathrm{I}}, \sigma_{x0}$ | $\sigma_{y\mathrm{I}}, \sigma_{y0}$	measured stresses inside and outside corrugated sheets
σ_0	yield stress of the material
β	aspect ratio a/b
θ	fold angle of corrugation
ϕ	angle between corrugation and mean plane of plate

Appendix II

Changes in Wavelength of a Stiffened Plate After Buckling

Consider a plate, under uniform edge stress, σ, whose deflected shape is of the form

$$\omega = \delta \cos\frac{\pi x}{a} \cos\frac{\pi y}{b}, \tag{a}$$

where a is the half wavelength.

The strain energy is:

$$U_1 = \frac{\pi^4}{8ab} D_1 \left[\left(\frac{b}{2}\right)^2 + \left(\frac{a}{b}\right)^2 \frac{D_2}{D_1} + 4\frac{G_{xy} I_{xy}}{D_1}\right] \delta^2 \tag{b}$$

and the work done by the load is

$$W = -\frac{\pi^2}{8} \frac{b}{a} \sigma t' \delta^2. \tag{c}$$

A membrane stress is assumed

$$\sigma_m = \sigma^0 \cos\frac{\pi y}{b}\cos\frac{2\pi x}{a}. \tag{d}$$

If the edges remain straight, then the shortening due to compression equals the lengthening due to tension minus the difference between the arc and chord lengths, i.e.,

$$\frac{\pi^2\delta^2}{4b} - \frac{2}{\pi}\sigma^0\frac{b}{E_y} = \frac{2\sigma^0 b}{\pi E_y},$$

$$\sigma_0 = \frac{\pi^3}{16}E_y\left(\frac{\delta}{b}\right)^2.$$

The strain energy due to membrane stress is:

$$U_2 = t'\int_{-b/2}^{b/2}\int_{-a/2}^{a/2}\frac{\sigma_m^2}{2E_y}dx\,dy = \frac{t'}{2E_y}\frac{\pi^3}{16}\left(\frac{\delta}{b}\right)^2 E_y^2\int_{-b/2}^{b/2}\int_{-a/2}^{a/2}\cos\frac{\pi y}{b}\cos\frac{2\pi x}{a}dx\,dy$$
$$= \frac{\pi^6 E_y}{204\,B}ab\left(\frac{\delta}{b}\right)^4 t'. \tag{e}$$

Using $W = U_1 + U_2$ gives

$$\sigma = \frac{\pi^2 D_1}{b^2 t'}\left[\left(\frac{b}{a}\right)^2 + \left(\frac{a}{b}\right)^2\frac{D_2}{D_1} + 4\frac{G_{xy}I_{xy}}{D_1}\right] + \frac{\pi^4 E_y}{256}\frac{a^2}{b^4}\delta^2\left(\frac{t}{t'}\right),$$

let $\delta = kb$, $a/b = K$

$$\sigma = \frac{\pi^2 D_1}{b^2 t'}\left[\frac{1}{K^2} + K^2\frac{D_2}{D_1} + 2\frac{D_3}{D_1}\right] + \frac{\pi^4 E_y}{256}(K)^2(k)^2\frac{t}{t'}$$

for σ_{min},
$$\frac{\partial\sigma}{\partial K} = 0$$

or
$$\left(\frac{D_2}{D_1} - \frac{1}{K^4}\right) + \frac{\pi^2 E_y}{256}\frac{b^2}{D_1}k^2 t = 0$$

or
$$K^4 = \frac{D_1}{D_2 + \frac{\pi^2}{256}E_y b^2 k^2 t}.$$

The assumption made in this investigation i.e. $\frac{a}{b} = \beta = \sqrt[4]{\frac{D_1}{D_2}}$, is acceptable in the case of corrugated plates since β is equal to K if E_y is small.

The foregoing analysis assumes that the axial compressive stress remains uniform. The fact that the axial stress varies across the plate does not change the preferred wavelength for a given deflection.

References

1. SHERBOURNE, A. N. and KOROL, R. M.: "Ultimate Strength of Plates in Uniaxial Compression." Preprint No. 1386, ASCE National Structural Engr. Meeting, Baltimore, April 1971.
2. TIMOSHENKO, S. P.: "Theory of Elastic Stability." McGraw-Hill Book Company, Inc., New York, 1961.

Summary

An investigation is made to ascertain the buckling and post-buckling characteristics of plates with different orthogonal rigidities, the load being applied in the stronger direction. The energy method is applied in computing the elastic, post-buckling loading line and an approach from column theory is utilized to obtain an approximate solution to plastic post-buckling behaviour of the plate.

Square tubes, formed from four corrugated plates joined along vertical edges, were used in the experiments. Each wall was considered as simply supported and, due to symmetry of deformation, each corner of the tube behaved as a hinge over its entire length. A tube, formed of flat sheets stiffened longitudinally, was also tested to show the influence of transverse membrane stress on post-buckling behaviour in contrast to corrugated sheets which could only sustain small transverse membrane forces.

Résumé

Pour le contrôle des caractéristiques de comportement lors du voilement et après-voilement sur des plaques à rigidité rectangulaires différentes, une examination est faite en admettant qu'une charge agisse dans le sens de la plus grande rigidité. On applique la méthode d'énergie en calculant la ligne de charge élastique d'après-voilement, et une méthode approchée de la théorie des piliers est employée afin d'obtenir une solution approchée du comportement plastique après-voilement de la tôle.

Pour les essais on a utilisé une forme de tubes carrés renforcés et assemblés le long des arêtes verticales. Chaque paroi du tube a été considérée comme reposant sur un appui-simple et, à la suite de la symétrie de déformation, chaque angle du tube se comportait comme une articulation sur toute la longueur. Un tube composé de tôles plates étayées longitudinalement a aussi été examiné, afin de démontrer l'influence de la sollicitation transversale de la membrane sur le comportement vis-à-vis des tubes à nervures qui ne peuvent transmettre que de petites forces transversales de membrane.

Zusammenfassung

Zur Nachprüfung der Charakteristiken des Beulungs- und Nachbeulungsverhaltens an Platten mit verschiedenen rechtwinkligen Steifigkeiten wird eine Untersuchung unter Annahme einer Belastung in der stärkeren Richtung angestellt. Die Energiemethode wird durch Kalkulieren der elastischen Nachbeul-Belastungslinie angewandt und eine Näherung aus der Stützentheorie benützt, um eine approximative Lösung zum nachgiebigen Nachbeulverhalten des Bleches zu erhalten.

Für die Versuche dienten quadratische aus 4 gerippten, längs der vertikalen Ecken zusammengefügte rohrähnliche Gebilde. Jede Wand wurde als einfach unterstützt betrachtet und, zufolge der Symmetrie der Deformation, verhielt sich jede Ecke des «Rohres» wie ein Gelenk über die ganze Länge. Ein Rohr, das aus flachen, longitudinalen versteiften Blechen gebildet war, wurde ebenfalls getestet, um den Einfluss der transversalen Membranbeanspruchung auf das Nachbeulverhalten im Gegensatz zu gerippten Rohren zu zeigen, die nur geringe transversale Membrankräfte aufnehmen können.

Leere Seite
Blank page
Page vide